

See discussions, stats, and author profiles for this publication at: <https://www.researchgate.net/publication/334039520>

# NONLINEAR DYNAMIC ANALYSIS PROCEDURE WITH LIMITED NUMBER OF ANALYSES AND SCALING

Conference Paper · June 2019

DOI: 10.7712/120119.6972.19723

CITATION

1

READS

468

4 authors:



**Andrea Miano**

University of Naples Federico II

35 PUBLICATIONS 259 CITATIONS

[SEE PROFILE](#)



**F. Jalayer**

University of Naples Federico II

112 PUBLICATIONS 3,174 CITATIONS

[SEE PROFILE](#)



**Hossein Ebrahimian**

University of Naples Federico II

42 PUBLICATIONS 473 CITATIONS

[SEE PROFILE](#)



**Andrea Prota**

University of Naples Federico II

513 PUBLICATIONS 5,787 CITATIONS

[SEE PROFILE](#)

Some of the authors of this publication are also working on these related projects:



Shear strengthening of masonry panels with inorganic composites [View project](#)



PE 2014–2016; joint program DPC-Reluis Task 3.3: Reparability limit state and damage cumulated effects [View project](#)

## NONLINEAR DYNAMIC ANALYSIS PROCEDURE WITH LIMITED NUMBER OF ANALYSES AND SCALING

A. Miano<sup>1</sup>, F. Jalayer<sup>1</sup>, H. Ebrahimian<sup>1</sup>, and A. Prota<sup>1</sup>

<sup>1</sup>) Department of Structures for Engineering and Architecture, University of Naples “Federico II”  
Via Claudio 21, 80125, Naples, Italy  
{andrea.miano, fatemeh.jalayer, ebrahimian.hossein, a.prota}@unina.it

---

### Abstract

*Incremental dynamic analysis (IDA) is the most frequently used non-linear dynamic analysis procedure for seismic fragility assessment. Nevertheless, its implementation involves complications such as heavy computational burden and potential bias in the results due to excessive scaling of the ground motion records. Cloud Analysis is an alternative nonlinear dynamic analysis procedure based on the structural response to as-recorded ground motions. Cloud Analysis does not suffer from the above-mentioned complications for IDA; however, it may lead to results that reveal too much sensitivity to the choice of the ground motion records. A novel hybrid nonlinear dynamic analysis procedure referred to as “Cloud to IDA” exploits the predictive capacity provided by Cloud Analysis to perform Incremental Dynamic Analysis (IDA) in a very efficient manner and with very little amount of scaling --without any loss of accuracy with respect to IDA. The procedure adopts as a systemic damage measure the critical demand to capacity ratio (DCR). This facilitates to a great extent identification of the intensity values at the onset of the limit state (where DCR is equal to unity by definition) and thereby the implementation of the IDA procedure. Cloud to IDA procedure is applied to the transverse perimeter frame of an older seven-storey reinforced concrete building in Van Nuys, US. This frame is modeled in OpenSees with fiber sections considering flexural-shear-axial interactions and bar slip due to fixed-end rotations. The proposed Cloud to IDA leads to results that are identical to IDA, when the same set of records are used. All of this is possible with a number of analyses that is sensibly lower with respect to IDA.*

**Keywords:** Cloud Analysis, Incremental dynamic analysis (IDA), nonlinear dynamic analyses, performance-based earthquake engineering, seismic fragility.

---

## 1 INTRODUCTION

Many existing reinforced concrete (RC) moment-resisting frame buildings in regions with high seismicity are particularly vulnerable to seismic excitation. Identifying accurately the level of performance can facilitate efficient seismic assessment of these buildings [1]. Analytic structural fragility assessment is one of the fundamental steps in the modern performance-based engineering [2]. There are alternative procedures available in the literature for characterizing the relationship between Engineering Demand Parameters (EDPs) and Intensity Measures (IMs) and performing fragility calculations based on recorded ground motions, such as, the Incremental Dynamic Analysis (IDA, [3, 4]), the Multiple-Stripe Analysis (MSA, see [5, 6]) and the Cloud Analysis (CA, [7-14]). The IDA is arguably the most frequently used non-linear dynamic analysis procedure. However, the application of IDA can be quite computationally demanding as the non-linear dynamic analyses are going to be repeated by scaling the ground motions to increasing levels of IM. It can be particularly useful to reduce both the computational effort within the IDA procedure while keeping almost the same level of accuracy. In such context, different approximate methods have emerged. These methods usually encompass schemes to perform nonlinear dynamic analyses of an equivalent simple SDOF model [15-16]. In addition, Vamvatsikos and Cornell [5, 6] have proposed the hunt & fill algorithm, that ensures the record scaling levels to be appropriately selected to minimize the number of required runs. A progressive IDA procedure has been proposed for optimal selection of records from an ensemble of ground-motions in order to predict the median IDA curve [17, 18]. Dhakal et al. [19] strived to identify in advance those ground motion records that are the best representatives for the prediction of a median seismic response. On the other hand, [20, 21] suggest that excessive scaling of records within the IDA procedure may lead to ground motion wave-forms whose frequency content and duration might not represent the corresponding intensity level. This might manifest itself in terms of a bias [22] in the IDA-based fragility curve with respect to fragility curves obtained based on no scaling or spectral-shape-compatible scaling [23-25].

Adopting an IM (intensity measure)-based fragility definition facilitates the implementation of the IDA analysis, which is usually carried out by adopting the maximum inter-story drift ratio as the structural response parameter. That is, the structural fragility can be also interpreted as the Cumulative Distribution Function (CDF) for the intensity values corresponding to the onset of the prescribed limit state. The main advantage of adopting this definition, in the context of IDA, is that one can stop the upward scaling of a record after the first excursion of the limit state. Liberally inspired from the code-based definition of demand to capacity ratios evaluated at the local level [26] for safety-checking purposes, the critical demand to capacity ratio, denoted as  $DCR_{LS}$ , that takes the structure closest to the onset of a prescribed limit state LS is adopted as the performance variable herein. This performance variable has been proposed as an effective and rigorous way of mapping the local structural behavior to the global level [36]. It has been shown [9-10, 27-31] that adopting  $DCR_{LS}$  as structural damage measure/performance variable facilitates the determination of the onset of a given limit state.  $DCR_{LS}$  is --by definition-- equal to unity at the onset of the limit state. Thus, adopting  $DCR_{LS}$  as the performance variable and plotting the IDA curves in terms of such variable facilitates the identification of intensity values corresponding to the onset of limit state as the intensity values corresponding to a  $DCR_{LS}$  equal to unity through the IDA curves. Adopting  $DCR_{LS}$  as the performance variable, an IDA curve can be obtained with only two data points consisting of pairs of intensity versus critical  $DCR_{LS}$ . It is most desirable that the interval of values covered by the two points includes the demand to capacity ratio equal to one --to avoid extrapolation for estimating the intensity level corresponding to the onset of the limit state. Based on

such a premise, an efficient solution for performing IDA is presented herein in which the intensity levels to scale to are chosen strategically to perform the minimum number of analyzes and minimum amount of scaling strictly necessary. To this end, one can exploit the simple linear (logarithmic) regression predictions made based on the results of the structural analysis to the un-scaled registered records to identify the range of intensity values near  $DCR_{LS}$  equal to unity. This procedure, which is coined herein as “Cloud to IDA”, delivers IM-based fragility curves by exploiting IDA curves constructed with minimum amount of scaling and minimum number of analyses strictly necessary. These fragility curves are shown later to be remarkably close to those obtained based on the IDA procedure.

This paper uses, as the numerical example, the transverse frame of a seven-story existing RC building in Van Nuys, CA. The frame is modeled in Opensees [32] by considering the flexural-shear-axial interactions in the columns. Being an older reinforced concrete frame, the column members are potentially sensitive to shear failure during earthquakes. Hence, a non-linear model is used to predict the envelope of the cyclic shear response [33, 34]. In addition, the fixed-end rotations due to bar slip are also considered in the estimation of the total lateral displacement of the members. The first-mode spectral acceleration denoted as  $Sa(T_1)$  is adopted as the intensity measure in this work.

## 2 METHODOLOGY

### 2.1 The structural performance variable

The critical demand to capacity ratio for a prescribed limit state [10-11, 14, 27] and denoted as  $DCR_{LS}$ , has been adopted as a proxy for the structural performance variable (DV). This DV is going to be convoluted directly with the intensity measure (IM) to estimate the seismic risk in the performance-based earthquake engineering framework.  $DCR_{LS}$  is defined as the demand to capacity ratio for the component or mechanism that brings the system closer to the onset of limit state LS (herein, the near-collapse limit state).  $DCR_{LS}$ , which is always equal to unity at the onset of limit state, is defined as:

$$DCR_{LS} = \max_l^{N_{mech}} \min_j^{N_l} \frac{D_{jl}}{C_{jl}(LS)} \quad (1)$$

where  $N_{mech}$  is the number of considered potential failure mechanisms;  $N_l$  the number of components taking part in the  $l^{th}$  mechanism;  $D_{jl}$  is the demand evaluated for the  $j^{th}$  component of the  $l^{th}$  mechanism;  $C_{jl}(LS)$  is the limit state capacity for the  $j^{th}$  component of the  $l^{th}$  mechanism. In this work, the critical demand to capacity ratio is going to be evaluated for the near-collapse limit state of the European Code [35]. The component demand to capacity ratios are expressed in terms of the maximum component chord rotation. This leads to a deformation-based  $DCR_{LS}$ . The maximum chord rotation demand  $D_{jl}$  for the  $j^{th}$  component of the  $l^{th}$  mechanism is obtained based on the results of the nonlinear dynamic analysis. The component chord rotation capacity  $C_{jl}(LS)$  for the  $j^{th}$  component of the  $l^{th}$  mechanism corresponds to the component capacity for the designated limit state regarding the specific failure mechanism. For the near-collapse limit state, it is defined as the point on the softening branch of the backbone curve in term of force-deformation of the component, where a 20% reduction in the maximum strength takes place. Moreover, it is to note that, when predicting non-linear response of structures for an ultimate limit state, it is common to encounter a few records leading to global “Collapse”; i.e., very high global displacement-based demands or non-convergence problems in the analyzing software. Obviously,  $DCR_{LS} > 1$  for the near-collapse limit state does not necessarily imply the occurrence of global Collapse. Herein, the global Collapse of the structure is identified as presented in [28].

## 2.2 Record selection criteria

Record selection for fragility analysis should reflect the dominant ground motion source mechanisms and the site conditions (see e.g. [36]). With respect to CA, there are a few relatively simple criteria to consider for selecting records for CA when adopting  $DCR_{LS}$  as the performance variable (see [9, 10] for more details). In the first place, the selected records should cover a vast range of intensity values. This helps in reducing the error in the estimation of the regression slope. It is also quite important to make sure that a significant portion of the records (there is no specific rule, say more than 30%) have  $DCR_{LS}$  values greater than unity. This recommendation aims at providing enough data points in the region of interest (i.e., vicinity of  $DCR_{LS}$  equal to unity). Finally, it is important to avoid selecting too many records (say more than 10% of total number of records) from the same earthquake.

As far as it regards the record-selection criteria for IDA procedure, as highlighted in [3], the number of records should be sufficient to capture the record-to-record variability in structural response. Previous studies [4] have assumed that for mid-rise buildings, 20 to 30 records are usually enough to provide sufficient accuracy in the estimation of seismic demands, for an IM like first-mode spectral acceleration,  $S_a(T_1)$ . Furthermore, a careful selection of ground motion records could be avoided if the adopted IM was sufficient (e.g., [20]). On the other hand, if the adopted IM was not sufficient (see [37-39] for alternative definitions/interpretations of sufficiency), the selected records at any given ground motion intensity level should ideally reflect the expected dominant ground motion characteristics. The record selection for IDA procedure can also be done so that it represents a dominant earthquake scenario identified by a magnitude and distance bin (see e.g., [4, 6]). It is to keep in mind that the accuracy of IDA procedure somehow depends on avoiding excessive scaling. Current literature [20, 21] suggests making sure that the frequency content of the scaled records is still (roughly) representative of the intensity to which they are scaled. This criterion might not be satisfied for records selected based on criteria recommended for CA –as it is desirable that they cover a wide range of intensity levels. The Cloud to IDA procedure can benefit from the information provided by the CA to ensure that the records are not scaled excessively. The procedure can avoid the potential scaling bias [22] sometimes attributed to IDA results.

## 2.3 Structural fragility assessment

Fragility estimation based on *Cloud to IDA* is compared with alternative non-linear dynamic analysis procedures such as Cloud Analysis considering the collapse cases ([11, 13-14], herein called Modified Cloud Analysis, MCA) and IDA. This section describes briefly fragility assessment based on these alternative methods.

The Cloud data encompasses pairs of ground motion *IM*, herein  $S_a(T_1)$  (referred to as  $S_a$  for brevity), and its corresponding structural performance variable  $DCR_{LS}$  for a set of ground-motion records. For ultimate limit states, a portion of the records may induce collapse. Let the Cloud data be partitioned into two parts: (a) *NoC* data which correspond to that portion of the suite of records for which the structure does not experience “Collapse”, (b) *C* corresponding to the “Collapse”-inducing records. The structural fragility for a prescribed limit state *LS* can be expanded with respect to *NoC* and *C* sets using Total Probability Theorem [6, 40]:

$$P(DCR_{LS} > 1 | S_a) = P(DCR_{LS} > 1 | S_a, NoC) \cdot (1 - P(C | S_a)) + P(DCR_{LS} > 1 | S_a, C) \cdot P(C | S_a) \quad (2)$$

where  $P(DCR_{LS} > 1 | S_a, NoC)$  is the conditional probability that  $DCR_{LS} > 1$ , given that “Collapse” has not taken place (*NoC*) and can be described by a Lognormal distribution [6, 11]:

$$P(DCR_{LS} > 1 | S_a, NoC) = \Phi \left( \frac{\ln \eta_{DCR_{LS} | S_a, NoC}}{\beta_{DCR_{LS} | S_a, NoC}} \right) = \Phi \left( \frac{\ln(a \cdot S_a^b)}{\beta_{DCR_{LS} | S_a, NoC}} \right) \quad (3)$$

where  $\eta_{DCR_{LS}|S_a, NoC}$  and  $\beta_{DCR_{LS}|S_a, NoC}$  are conditional median and standard deviation (dispersion) of the natural logarithm of  $DCR_{LS}$  for  $NoC$  portion of the data (calculated as per Eqs 2 and 3 applied to the  $NoC$  portion of the collapse data, respectively). For the rest of this manuscript, the conditioning on  $NoC$  is dropped for brevity and they are referred to as  $\eta_{DCR_{LS}|S_a}$  and  $\beta_{DCR_{LS}|S_a}$ . The term  $P(DCR_{LS} > 1 | S_a, C)$  is the conditional probability of that  $DCR_{LS}$  is greater than unity given ‘‘Collapse’’. This term is equal to unity, i.e., in the cases of ‘‘Collapse’’, the limit state  $LS$  (herein, near-Collapse) is certainly exceeded. Finally,  $P(C|S_a)$  in Eq. 2 is the probability of collapse, which can be predicted by a logistic regression model (a.k.a., logit) as a function of  $S_a$  (see also [11, 13]), and expressed as follows:

$$P(C|S_a) = \frac{1}{1 + e^{-(\alpha_0 + \alpha_1 \cdot \ln S_a)}} \quad (4)$$

where  $\alpha_0$  and  $\alpha_1$  are the parameters of the logistic regression.

The structural fragility based on IDA, instead, is expressed, in an  $IM$ -based manner, as the cumulative distribution function for the  $IM$  values that mark the limit state threshold. Taking advantage of the  $IM$ -based fragility definition and assuming that the critical spectral acceleration values at the onset of the limit state denoted by  $S_a^{DCR=1}$  are Lognormally distributed, the structural fragility based on IDA analysis can be calculated as:

$$P(DCR_{LS} > 1 | S_a) = P(S_a^{DCR=1} < S_a) = \Phi \left( \frac{\ln S_a - \ln \eta_{S_a^{DCR=1}}}{\beta_{S_a^{DCR=1}}} \right) \quad (5)$$

where  $\eta_{S_a^{DCR=1}}$  and  $\beta_{S_a^{DCR=1}}$  are the median and (logarithmic) standard deviation of  $S_a^{DCR=1}$ .

Finally, to compare the fragility curves obtained based on alternative non-linear analysis procedures and suites of ground motion records of different sizes, it is desirable to find a way for quantifying the uncertainty in the evaluation of structural fragility. This is done herein by employing the concept of *Robust Fragility* to define a prescribed confidence interval for the estimated fragility curve. The *Robust Fragility* [10-11] is defined as the expected value for a prescribed fragility model considering the joint probability distribution for the (fragility) model parameters  $\chi$ . The *Robust Fragility*, by using Total Probability Theorem, is written as:

$$P(DCR_{LS} > 1 | S_a, \mathbf{D}) = \int_{\Omega_\chi} P(DCR_{LS} > 1 | S_a, \chi) f(\chi | \mathbf{D}) d\chi = \mathbf{E}_\chi [P(DCR_{LS} > 1 | S_a, \mathbf{D}, \chi)] \quad (6)$$

where  $\chi$  is the vector of fragility model parameters and  $\Omega_\chi$  is its domain;  $f(\chi | \mathbf{D})$  is the joint probability distribution for fragility model parameters given the vector of data  $\mathbf{D}$ . The term  $P(DCR_{LS} > 1 | S_a, \chi)$  is the fragility model given that the vector  $\chi$  is known. Note that it has been assumed that the vector  $\chi$  is sufficient to describe the data.  $\mathbf{E}_\chi(\cdot)$  is the expected value over the vector of fragility parameters  $\chi$ . Based on the definition represented in Eq. 6, the variance  $\sigma^2$  in fragility estimation can be calculated as:

$$\sigma^2 [P(DCR_{LS} > 1 | S_a, \mathbf{D}, \chi)] = \int_{\Omega_\chi} P(DCR_{LS} > 1 | S_a, \chi)^2 f(\chi | \mathbf{D}) d\chi - \mathbf{E}_\chi^2 [P(DCR_{LS} > 1 | S_a, \mathbf{D}, \chi)] \quad (7)$$

## 2.4 Cloud to IDA procedure

The *Cloud to IDA* procedure derives IDA-based fragility curves by obtaining the  $S_a$  values corresponding to unity denoted as  $S_a^{DCR=1}$ . This is done with efficiency by obtaining IDA curves with few points. The flowchart in Fig. 1 provides a step-by-step guide to *Cloud to IDA*:  
1- Establish an original record selection for MCA. One might choose records based on criteria suggested specifically for MCA as in [11]. Otherwise one can use an established set of records such as the ones proposed by FEMA [41].

2- Perform structural analysis, obtaining Cloud data points. Identify  $NoC$  and  $C$  data.

- 3- (Optional) Scale down the C data and merge them together with the *NoC* data.
- 4- Fit a linear regression in the logarithmic scale to the non-collapse portion of the Cloud data (that may include scaled down C data). Identify  $S_{a,Cloud}^{DCR=1}$  as the spectral acceleration corresponding to  $DCR_{LS}=1$  by the regression prediction.
- 5- Define prescribed confidence intervals around  $S_{a,Cloud}^{DCR=1}$  and  $DCR_{LS}=1$ . This leads to the identification of box-shaped area. The records that lie within this area can be selected as the records suitable for next steps of the *Cloud to IDA* procedure.
- 6- Scale all the records thus-obtained to (a value slightly larger or smaller than) the spectral acceleration value  $S_{a,Cloud}^{DCR=1}$ . For those records, that are to the right of the regression prediction, the spectral acceleration value to scale to is going to be slightly smaller than  $S_{a,Cloud}^{DCR=1}$  and vice versa. This step provides the second point of IDA curve for all the records.
- 7- Connect the two points in order to obtain the IDA lines. Find the projected  $S_a^{DCR=1}$  values as the intersection of the IDA lines (or their extension to the left or right) with  $DCR_{LS}=1$ .
- 8- Scale all the records to  $S_a^{DCR=1}$  values to obtain the third data point on the IDA curves.
- 9- Check if the value  $DCR_{LS}=1$  falls within one of the IDA line segments and obtain the corresponding  $S_a^{DCR=1}$  value through interpolation.
- 10- Repeat steps 8 and 9 for those records in which the value  $DCR_{LS}=1$  falls completely to one side of the IDA line segments obtained so far.

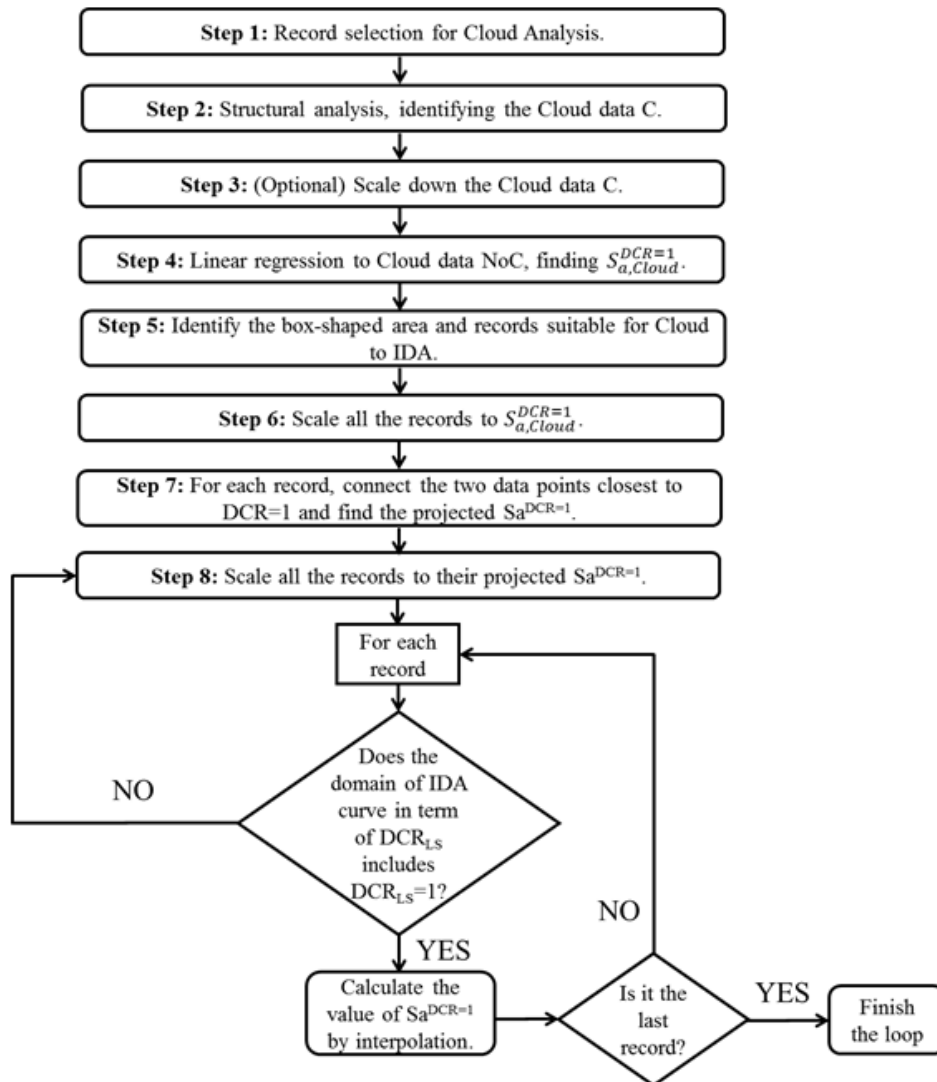


Figure 1. Flowchart for *Cloud to IDA* procedure.

### 3 NUMERICAL APPLICATION

#### 3.1 Building description and modeling

A perimeter transverse frame of the seven-story hotel building in Van Nuys, California, is modeled and analyzed in this study (see [14] for the geometrical details of the frame). The building is located in the San Fernando Valley of Los Angeles County (34.221° north latitude, 118.471° west longitude). The frame building was designed in 1965 according to the 1964 Los Angeles City Building Code, and constructed in 1966. The building was severely damaged in the M6.7 1994 Northridge earthquake. All the column and beam reinforcement and mechanical material properties details are provided in [11, 14, 30, 42-44]. The axial/flexural behavior in beam-column elements is modeled based on distributed plasticity using different integration techniques. The shear behavior is modeled as a zero-length element in column end aggregated in series with the flexural element. The estimation of shear backbone is described comprehensively in [33] (see also [30] for more details). Moreover, the rigid-end rotation due to bar slip is modeled as two zero-length elements at the ends of the columns (see [45] for the calculation of slip force displacement backbone). The total lateral response of a RC column is, then, modeled using a set of springs in series in OpenSees (the flexural spring is the fiber section element). The flexure, shear and bar slip deformation models are modeled by springs in series. The three deformation components are added together to predict the total response up to the peak strength of the column. Rules are established for the post-peak behavior of the springs based on a comparison of the shear strength  $V_n$ , the yield strength  $V_y$ , and the flexural strength  $V_p$ . By comparing  $V_n$ ,  $V_y$ , and  $V_p$ , the columns are classified into different categories [33], to determinate if they are shear critical, shear-flexural critical or flexural critical. Most of the columns of the case-study frame are classified as shear critical. However, the explicit modeling of the behavior of the masonry infills present in three spans in the ground story of the modeled frame is herein neglected [46].

#### 3.2 Modified Cloud Analysis (MCA)

First of all, it is to note that the set of records presented in FEMA P695 [41] is used for the MCA and IDA. The FEMA set [14] includes twenty-two far-field records and twenty-eight near-field records. With reference to the twenty-eight near-field records, fourteen records are identified as “pulse-like”. Only one horizontal component of each record has been selected. The FEMA suite of records covers a range of magnitudes between 6.5 and 7.9, and closest distance-to-ruptured area (denoted as  $R_{RUP}$ ) up to around 30 km.

Fig. 2a shows the scatter plots for Cloud data based on the ground motion records listed in the FEMA record set (colored squares). The cyan-colored squares represent the *NoC* data, while only one record out of fifty ground motions causes collapse or global dynamic instability (*C* data) as shown with a red-colored square. The MCA regression model (i.e., regression prediction, the estimated regression parameters, and the standard error of regression as described in Section 2) fitted to the *NoC* data is shown on the figure. The black solid line represents the regression prediction  $\eta_{DCR_{LS} | S_a}$  which can be interpreted as the 50<sup>th</sup> percentile (a.k.a., median)  $DCR_{LS}$  given spectral acceleration conditioned on *NoC*. The line  $DCR_{LS}=1$  corresponding to the onset of near-collapse limit state is shown with red-dashed line. It can be seen that the MCA data not only covers a vast range of spectral acceleration values, but also provides numerous data points in the vicinity of  $DCR_{LS}=1$ . The horizontal black dash-dotted line indicates the spectral acceleration  $S_{a,Cloud}^{DCR=1}=(1/a)^{1/b}$  corresponding to  $DCR_{LS}=1$  based on the regression prediction. Fig. 2b shows the fragility curves based on MCA (cyan dashed line) and the *Robust Fragility* with its two standard deviation confidence interval (plotted as black solid

line and the shaded area, based on MCA as described in Section 2). The figure also illustrates the conditional probability of collapse given intensity  $P(C|S_a)$  as in Eq. 4 and reports the logistic ( $\alpha_0$  and  $\alpha_1$ ) regression model parameters.

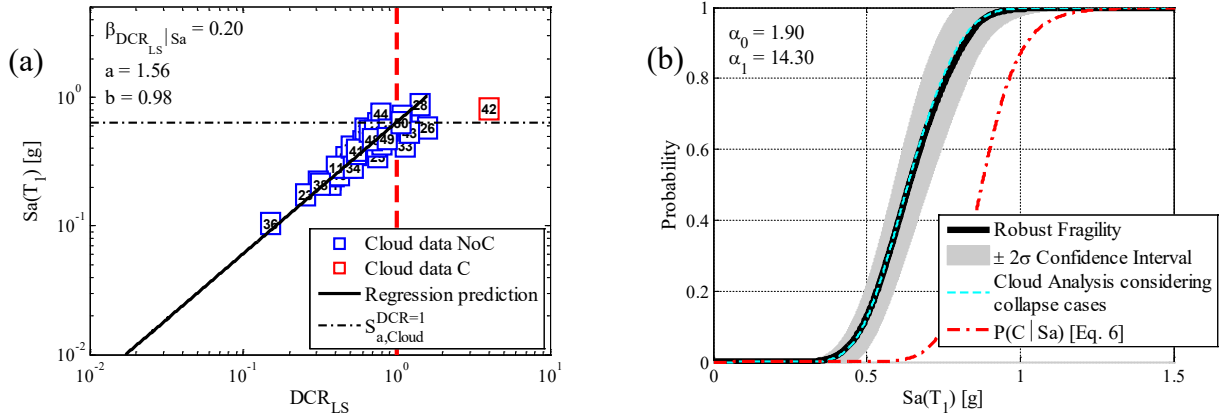


Figure 2: (a) Cloud data and regression, and (b) the fragility curves.

### 3.3 IDA Analysis

The IDA is performed for the suite of fifty FEMA ground-motion. The IDA curves are plotted in thin grey lines in Fig. 3a. Each curve shows the variation in the performance variable  $DCR_{LS}$  for a given ground-motion record as a function of  $S_a$  while the record's amplitude is linearly scaled-up. The grey dot at the end of each IDA curve denotes the ultimate  $S_a$  level before numerical non-convergence or global collapse is encountered (based on the criteria defined in Section 2). The  $S_a$  values on the IDA curves corresponding to  $DCR_{LS}=1$  and denoted as  $S_a^{DCR_{LS}=1}$  (i.e., the intensity levels marking the onset of the limit state) are shown as red stars. The histogram of  $S_a^{DCR_{LS}=1}$  values together with the fitted (Lognormal) probability density function (PDF), plotted as a black solid line, are shown in Fig. 3a. The horizontal thin black dash-dotted line represents the median of  $S_a^{DCR_{LS}=1}$ , which is denoted as  $\eta_{DCR_{LS}|S_a}$  and known as median spectral acceleration capacity. Fig. 3b shows the comparison between the Robust Fragilities and their plus/minus two standard deviation confidence intervals based on MCA (black solid line and the corresponding shaded area) and IDA (blue dotted line and the small blue dotted lines for identifying the confidence interval), as described in Sections 2. The difference between Cloud- and IDA-based fragilities is contained within a 2 standard deviation confidence band for both methods; with the IDA-based fragilities being on the more conservative side.

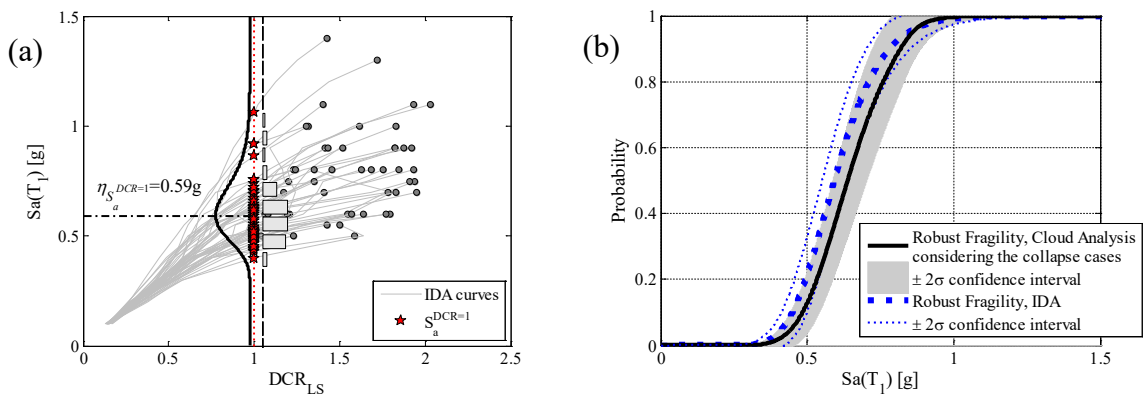


Figure 3: (a) the IDA curves and the spectral acceleration capacity values  $S_a^{DCR_{LS}=1}$ ; (b) Comparison between The fragility curves based IDA and MCA (Cloud Analysis considering the collapse cases).

### 3.4 Cloud to IDA procedure

The step-by-step *Cloud to IDA* procedure as described in the methodology section (see the flowchart in Fig. 1) is applied herein considering two reduced record sets obtained with the objective of limiting the scaling of ground motion records (*Reduced set 1* and *Reduced set 2* as described in the next paragraphs).

- The first step of the procedure is accomplished by choosing the FEMA record set as the original record selection for MCA.
- The second step is to perform structural analysis and to identify the collapse-inducing records (C and NoC data, only one case of collapse is identified herein).
- The step three of the procedure has been skipped (only one collapse case was identified).
- In the next step, a linear regression in the logarithmic scale is performed on the non-collapse portion of the Cloud data (Fig. 2a). At this point, the spectral acceleration at  $DCR_{LS}=1$ , i.e.  $S_{a,Cloud}^{DCR=1}$ , and the constant conditional logarithmic standard deviation of  $DCR_{LS}$  given  $S_a$  denoted as  $\beta_{DCR_{LS}|S_a}$ , as shown in Fig. 2a are calculated.
- The next step involves defining prescribed confidence intervals around  $S_{a,Cloud}^{DCR=1}$  and  $DCR_{LS}=1$  in order to identify the records that are going to be subjected to least amount of scaling (as predicted by the regression). Two suites of reduced record sets are selected from the pool of FEMA records:
  - *Reduced set 1*:  $N=10$  records that lie within the box defined by the plus/minus one (logarithmic) standard deviation stripes away from  $S_{a,Cloud}^{DCR=1}$  and  $DCR_{LS}=1$  (see Fig. 4a).
  - *Reduced set 2*:  $N=19$  records that lie within the box defined by the plus/minus one (logarithmic) standard deviations away from  $S_{a,Cloud}^{DCR=1}$  and plus/minus 1.5 (logarithmic) standard deviations away from  $DCR_{LS}=1$  (see Fig. 4b).

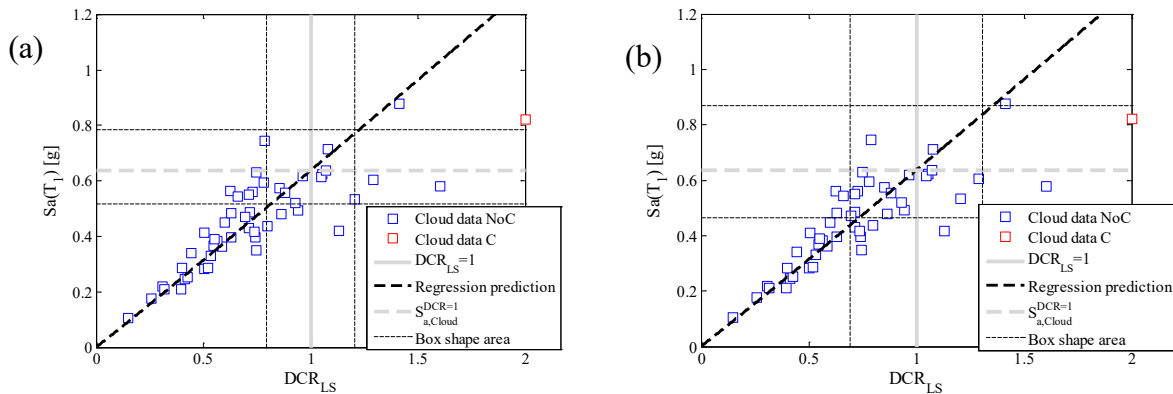


Figure 4: Box shape areas defining (a) *Reduced set 1*, and (b) *Reduced set 2*.

The *Cloud to IDA* procedure is described hereafter for the *Reduced set 2* ( $N=19$ , however the procedure is carried out for both record sets and the results are reported at the end of this section).

- In the next step, all the records within the rectangular area are scaled to (a value slightly larger or smaller than the) the spectral acceleration value  $S_{a,Cloud}^{DCR=1}$ . In case the scaled records become collapse-inducing, the spectral acceleration to scale to should be adjusted accordingly so that the scaled record does not lead to collapse (this might require some iteration). At the end of this step, IDA line segments for all the records can be obtained by connecting the two points.

- At this point a visual survey of whether the  $DCR_{LS}=1$  falls within the IDA lines or outside is performed. Fig. 5a shows the intersection/projection of the IDA lines and the value  $DCR_{LS}=1$  denoted as “projected”  $S_a^{DCR=1}$  for each record.
- The last step is to scale all the records to the “projected”  $S_a^{DCR=1}$  in order to obtain the third data point on the IDA curves. Note that the records can be scaled to a value slightly larger or smaller than the “projected”  $S_a^{DCR=1}$  (Fig. 5a). The obvious advantage of scaling the records to the projected intersection with unity is that it will lead to a third point on the IDA curve close to a  $DCR_{LS}=1$ . At this point, most probably, as in the case study in Fig. 5b, the  $S_a^{DCR=1}$  values can be calculated by interpolation for all the records (i.e., for all of the records a gray dashed line segment can be found). Finally, the fragility curve can be obtained based on the statistics of  $S_a^{DCR=1}$  values. In case there are still records for which the  $DCR_{LS}=1$  falls totally to the left or the right of the three points obtained so far, the previous step can be repeated until an IDA line segment including  $DCR_{LS}=1$  can be identified. In the case study, the  $S_a^{DCR=1}$  values are obtained for all the records based on only three IDA points.

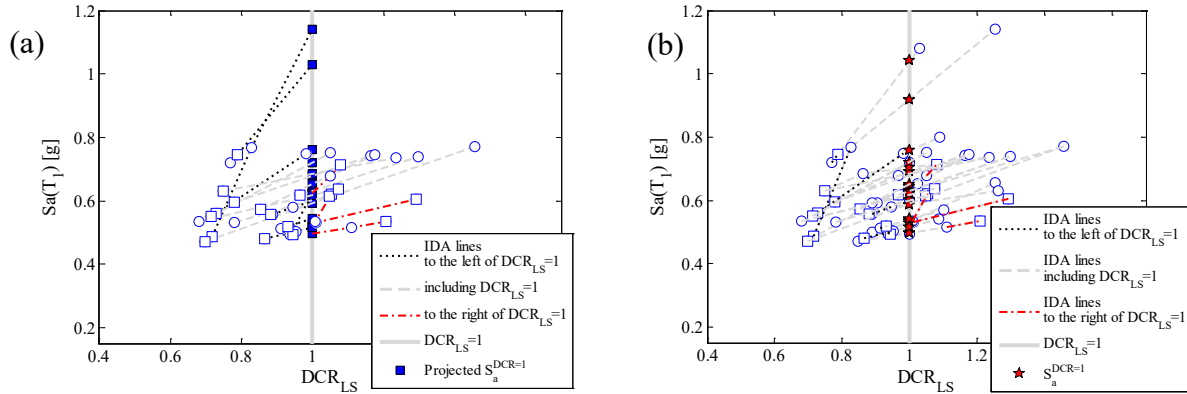


Figure 5. *Cloud to IDA* procedure: (a) the “projected”  $S_a^{DCR=1}$  values; (b) The resulting  $S_a^{DCR=1}$  values used to develop the *Cloud to IDA* fragility curve.

### 3.5 Results and discussions

Fig. 6a reported below shows the *Robust Fragility* curves and their plus/minus one standard deviation interval obtained by employing the *Cloud to IDA* procedure for *Reduced sets 1* and *2*, in red dashed lines of different thickness (thicker for *Reduced set 2* which is the larger set) and the corresponding confidence intervals are marked by thin red dashed lines of the different color shades (darker for *Reduced set 2* which is the larger set). Note that the *Robust Fragility* calculation for *Cloud to IDA* is the same as IDA as described in detail in [47-48]. The confidence band is clearly wider for the smaller record set (with only  $N=10$  records). Moreover, it can be seen that the *Robust Fragility* curves obtained based on the two sets of records are in close agreement (contained within the plus/minus one standard deviation interval of each other). Fig. 6b demonstrates the *Robust Fragility* curve and its plus/minus one standard deviations confidence interval based on the MCA in solid black line and a gray shaded area together with the *Robust Fragility* curves obtained through the *Cloud to IDA* procedure based on *Reduced sets 1* and *2* (red dashed lines of different thickness to reflect the size of the set). These two fragility curves are entirely contained inside the plus/minus one standard deviation of the *Robust Fragility* curve based on the MCA. Fig. 7 shows the comparison between the IDA and *Cloud to IDA* procedures for all the three record sets (*Reduced set 1*, and *2*, and *Complete*); the line types for each procedure are distinguished by their thickness: the larger the set of records the thicker the line). For each given record set, the fragility curves obtained based on IDA and *Cloud to IDA* procedures are almost identical. In the context of

this study, the *Cloud to IDA* procedure demonstrates its capability of improving the computational efficiency significantly without sacrificing the accuracy with respect to the original IDA method.

Table 1 shows the statistical parameters for the fragility curves, where  $\eta$  is the median value of the fragility curve and  $\beta$  is its logarithmic standard deviation. It also shows the number of analyses required for each of the alternative non-linear dynamic analysis procedures. Moreover, the table illustrates the mean annual frequencies of exceeding the near-Collapse limit state (i.e., risk) denoted by  $\lambda_{LS}$  corresponding to the *Robust Fragility* and the *Robust Fragility* plus/minus two standard deviations.  $\bar{R}_F$  denotes the risk obtained by integrating *Robust Fragility* and site-specific hazard;  $\bar{R}_{F\pm 2\sigma}$  denotes risk calculated by integrating *Robust Fragility* plus/minus its two-standard deviation and the site-specific hazard. The number of analyses required for implementing IDA procedure is equal to the product of the number of the records and the number of the intensity levels ( $50 \times 17$ ). As far as it regards the computational effort related to the implementation of *Cloud to IDA* procedure, the number of analyses required is not fixed. Herein, it is equal to the number of records required for MCA (i.e., 50) plus two times the number of the selected records ( $10 \times 2$  and  $19 \times 2$  for *Reduced sets 1* and *2*, respectively). It is to be mentioned that the IDA analysis herein has been done based on the same pool of original records as MCA and *Cloud to IDA*. Nevertheless, the IDA can be employed with a smaller pool of records than the one employed herein and the total number levels can be lower than the 17 levels employed herein (e.g., as low as 10). Overall, the *Cloud to IDA* fragilities with limited scaling (*Reduced sets 1* and *2*) provide very reasonable results with a sensibly lower analysis effort compared to IDA. However, the prize for the lowest number of analyses without any scaling goes to MCA.

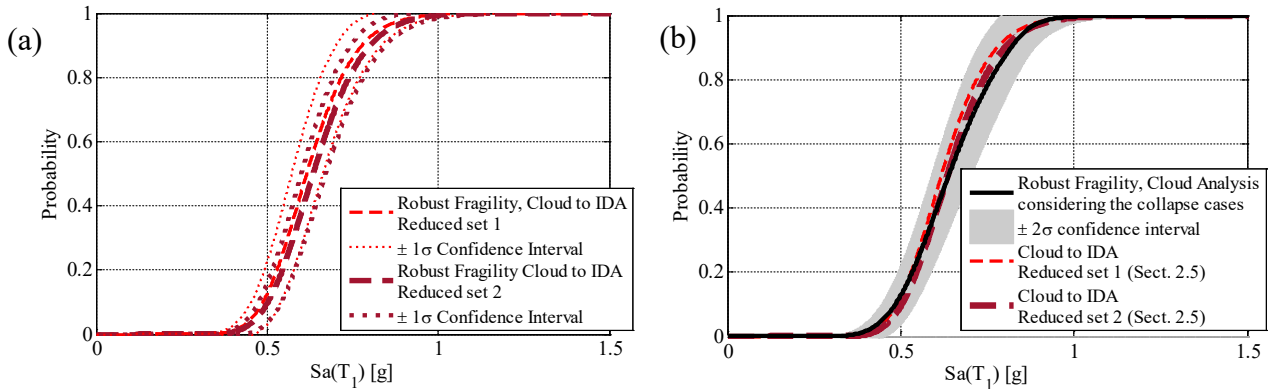


Figure 6: (a) *Robust Fragility* curves and their plus/minus one standard deviation intervals for *Reduced sets 1* and *2*; (b) MCA (Cloud Analysis considering the collapse cases) and its plus/minus two standard deviations confidence interval and *Robust Fragility* curves for the *Cloud to IDA* procedure and based on the two sets *Reduced sets 1* and *2*.

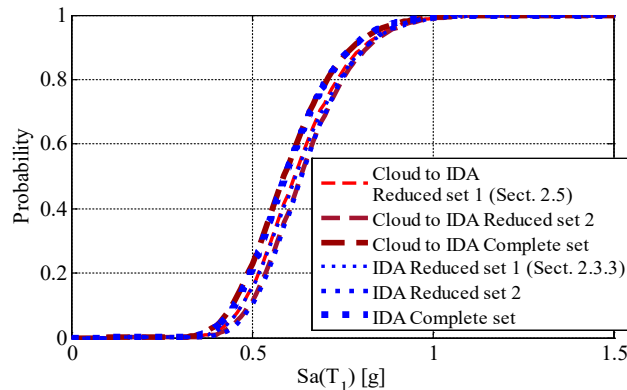


Figure 7: Comparison between IDA and *Cloud to IDA* for *Reduced sets 1* and *2*, and complete set (FEMA).

Table 1. Statistical parameters for fragility curves, number of analyses and mean annual frequencies of exceeding the limit state for the alternative nonlinear dynamic procedures

Methodology	$\eta$ [g]	$\beta$	Number of analyses	$\lambda_{LS}$ using the <i>Robust Fragility</i>		
				$\tilde{R}_{F-2\sigma}$	$\tilde{R}_F$	$\tilde{R}_{F+2\sigma}$
MCA (Complete set)	0.63	0.20	50	$1.9 \times 10^{-3}$	$2.5 \times 10^{-3}$	$3.1 \times 10^{-3}$
<i>Cloud to IDA Reduced set 1</i>	0.62	0.21	$50+10 \times 2=70$	$1.8 \times 10^{-3}$	$2.6 \times 10^{-3}$	$3.5 \times 10^{-3}$
<i>Cloud to IDA Reduced set 2</i>	0.63	0.20	$50+19 \times 2=88$	$1.8 \times 10^{-3}$	$2.4 \times 10^{-3}$	$3.1 \times 10^{-3}$
IDA (Complete set)	0.59	0.21	$50 \times 17=850$	$2.4 \times 10^{-3}$	$2.9 \times 10^{-3}$	$3.4 \times 10^{-3}$
<i>Cloud to IDA (Complete set)</i>	0.59	0.21	$50 \times 3+1=151$	$2.4 \times 10^{-3}$	$2.9 \times 10^{-3}$	$3.4 \times 10^{-3}$

#### 4 CONCLUSIONS

Cloud to IDA is proposed as an efficient procedure with limited scaling of ground motion records that exploits the results of a simple MCA for carrying out incremental dynamic analysis (IDA). The procedure is applicable when the adopted EDP is expressed in terms of a critical demand to capacity ratio that is equal to unity at the onset of the limit state. There is indeed a natural link between Cloud and IDA procedures. The Cloud data can be viewed as the first points on the various IDA curves. On the other hand, an IDA curve can be obtained theoretically with only two data points, consisted of pairs of intensity versus critical demand to capacity values, if the interval of values covered by the two points covers the demand to capacity ratio equal to one. In the Cloud to IDA procedure, the intensity levels to scale to are chosen strategically with the aim of performing the minimum number of analyzes and minimum amount of scaling necessary. To this end, one can exploit the simple linear (logarithmic) regression predictions made based on the results of the structural analysis to the un-scaled registered records to choose landmark IM levels for scaling. Those records that are going to be potentially scaled up/down by a factor close to unity are identified from the pool of original records in order to avoid excessive scaling of the records. The results indicate that the fragility and risk estimates obtained based on the *Reduced Sets 1* and *2* are very close to those obtained based on the MCA. This is while the IDA-based fragility reveals a slight shift to the left compared to the other more “scaling-conscious” methods. Nevertheless, the proposed Cloud to IDA leads to results that are identical to IDA, when the same set of records are used. All of this is possible with a number of analyses that is sensibly lower (almost an order of magnitude) with respect to IDA. It is worth emphasizing that the use of a performance variable in the demand to capacity ratio format (i.e., it is equal to unity at the onset of the prescribed limit state) as the performance variable directly is indispensable for the proposed Cloud to IDA procedure. For instance, the procedure can be applied even when the maximum inter-story drift is employed as the EDP. In such case, the adopted DM is equal to the ratio of the maximum inter-storey drift ratio demand to the maximum inters-storey drift ratio capacity for the desired limit state.

#### REFERENCES

- [1] F. Jalayer, L. Elefante, I. Iervolino, G. Manfredi, Knowledge-based performance assessment of existing RC buildings. *Journal of Earthquake Engineering*, **15(3)**, 362-389, 2011.
- [2] C.A. Cornell, H. Krawinkler, Progress and challenges in seismic performance assessment. *PEER Center News*, **3(2)**, 1-3, 2000.

- 
- [3] D. Vamvatsikos, C.A. Cornell, Incremental dynamic analysis. *Earthquake Engineering and Structural Dynamics*, **31(3)**: 491-514, 2002.
- [4] D. Vamvatsikos, C.A. Cornell, Applied incremental dynamic analysis. *Earthquake Spectra*, **20(2)**: 523-553, 2004.
- [5] F. Jalayer, C.A. Cornell, A Technical Framework for Probability-Based Demand and Capacity Factor Design (DCFD) Seismic Formats. *Pacific Earthquake Engineering Center (PEER) 2003/08*.
- [6] F. Jalayer, C.A. Cornell, Alternative non-linear demand estimation methods for probability - based seismic assessments. *Earthquake Engineering and Structural Dynamics*, **38(8)**: 951-972, 2009.
- [7] P. Bazzurro, C.A. Cornell, N. Shome, J.E. Carballo, Three proposals for characterizing MDOF nonlinear seismic response. *Journal of Structural Engineering ASCE*, **124(11)**: 1281-1289, 1998.
- [8] C.A. Cornell, F. Jalayer, R.O. Hamburger, D.A. Foutch, The probabilistic basis for the 2000 SAC/FEMA steel moment frame guidelines. *Journal of Structural Engineering ASCE*, **128(4)**: 526-533, 2002.
- [9] H. Ebrahimian, F. Jalayer, D. Asprone, A.M. Lombardi, W. Marzocchi, A. Prota, G. Manfredi, A performance-based framework for adaptive seismic aftershock risk assessment. *Earthquake Engineering and Structural Dynamics*, **43(14)**: 2179-2197, 2014.
- [10] F. Jalayer, R. De Risi, G. Manfredi, Bayesian Cloud Analysis: efficient structural fragility assessment using linear regression. *Bulletin of Earthquake Engineering*, **13(4)**: 1183-1203, 2015.
- [11] F. Jalayer, H. Ebrahimian, A. Miano, G. Manfredi, H. Sezen, Analytical fragility assessment using un-scaled ground motion records. *Earthquake Engineering and Structural Dynamics*, **46(15)**: 2639-2663, 2017.
- [12] H. Ebrahimian, F. Jalayer, D. Asprone, A.M. Lombardi, W. Marzocchi, A. Prota, G. Manfredi, An outlook into time-dependent aftershock vulnerability assessment. *Proceedings of 4<sup>th</sup> ECCOMAS Thematic Conference on Computational Methods in Structural Dynamics and Earthquake Engineering (COMPdyn)*, Kos, Greece, June 2013.
- [13] F. Jalayer, H. Ebrahimian, Seismic risk assessment considering cumulative damage due to aftershocks. *Earthquake Engineering and Structural Dynamics*, **46(3)**: 369-389, 2017.
- [14] A. Miano, F. Jalayer, H. Ebrahimian, A. Prota, Cloud to IDA: Efficient fragility assessment with limited scaling, *Earthquake Engineering and Structural Dynamics* **47(5)**, 1124-1147, 2018.
- [15] D. Vamvatsikos, C.A. Cornell, Direct estimation of seismic demand and capacity of multi degree-of-freedom systems through incremental dynamic analysis of single degree of freedom approximation. *Journal of Structural Engineering ASCE*, **131(4)**: 589-599, 2005.
- [16] M. Dolšek, P. Fajfar, Simplified non-linear seismic analysis of infilled reinforced concrete frames. *Earthquake Engineering and Structural Dynamics*, **34(1)**: 49-66, 2005.
- [17] A. Azarbakht, M. Dolšek, Prediction of the median IDA curve by employing a limited number of ground motion records. *Earthquake Engineering and Structural Dynamics*, **36(15)**: 2401-2421, 2007.

- 
- [18] A. Azarbakht, M. Dolšek, Progressive incremental dynamic analysis for first-mode dominated structures. *Journal of Structural Engineering ASCE*, **137(3)**: 445-455, 2010.
- [19] R.P. Dhakal, J.B. Mander, N. Mashiko, Identification of critical ground motions for seismic performance assessment of structures. *Earthquake Engineering and Structural Dynamics*, **35(8)**: 989-1008, 2006.
- [20] J.W. Baker, C.A. Cornell, A vector-valued ground motion intensity measure consisting of spectral acceleration and epsilon. *Earthquake Engineering and Structural Dynamics*, **34**: 1193-1217, 2005.
- [21] T. Lin, J.W. Baker, Introducing Adaptive Incremental Dynamic Analysis: A new tool for linking ground motion selection and structural response assessment. *Proceedings of the 11<sup>th</sup> International Conference on Structural Safety and Reliability (ICOSSAR), 2013*.
- [22] N. Luco, P. Bazzurro, Does amplitude scaling of ground motion records result in biased nonlinear structural drift responses? *Earthquake Engineering and Structural Dynamics*, **36(13)**: 1813-1835, 2007.
- [23] T. Lin, S.C. Harmsen, J.W. Baker, N. Luco, Conditional Spectrum computation incorporating multiple causal earthquakes and ground motion prediction models. *Bulletin of Seismological Society of America*, **103(2A)**: 1103-1116, 2013.
- [24] T. Lin, C.B. Haselton, J.W. Baker, Conditional spectrum - based ground motion selection. Part I: Hazard consistency for risk - based assessments. *Earthquake Engineering and Structural Dynamics*, **42(12)**: 1847-1865, 2013.
- [25] N. Jayaram, T. Lin, J.W. Baker, A computationally efficient ground-motion selection algorithm for matching a target response spectrum mean and variance. *Earthquake Spectra*, **27(3)**: 797-815, 2011.
- [26] ASCE/SEI 41-13. Seismic evaluation and retrofit of existing buildings. *American Society of Civil Engineers*: Reston, VA, 2014.
- [27] F. Jalayer, P. Franchin, P.E. Pinto, A scalar damage measure for seismic reliability analysis of RC frames. *Earthquake Engineering and Structural Dynamics*, **36(13)**: 2059-2079, 2007.
- [28] A. Miano, H. Sezen, F. Jalayer, A. Prota, Performance based assessment methodology for retrofit of buildings. *Journal of Structural Engineering ASCE, Accepted paper*, 2019.
- [29] H. Ebrahimian, F. Jalayer, G. Manfredi, Seismic retrofit decision-making of bridges based on life-cycle cost criteria. *Proceedings of the 5<sup>th</sup> ECCOMAS Thematic Conference on Computational Methods in Structural Dynamics and Earthquake Engineering (COMPDYN)*, Crete, Greece, May, 2015.
- [30] A. Miano, F. Jalayer, A. Prota, Cloud to Ida: A very efficient solution for performing incremental dynamic analysis. *Lecture Notes in Civil Engineering*. Volume 10, 2016, Pages 355-368.
- [31] A. Miano, F. Jalayer, A. Prota, Considering Structural Modeling Uncertainties using Bayesian Cloud Analysis. *Proceedings of the 6<sup>th</sup> ECCOMAS Thematic Conference on Computational Methods in Structural Dynamics and Earthquake Engineering (COMPDYN)*, Rhodes, Greece, 15-17 June 2017.

- 
- [32] F. McKenna, OpenSees: a framework for earthquake engineering simulation. *Computing in Science and Engineering*, **13(4)**: 58-66, 2011.
- [33] E.J. Setzler, H. Sezen, Model for the lateral behavior of reinforced concrete columns including shear deformations. *Earthquake Spectra*, **24(2)**: 493-511, 2008.
- [34] H. Sezen, Shear deformation model for reinforced concrete columns. *Structural Engineering and Mechanics*, **28(1)**: 39-52, 2008.
- [35] CEN. Eurocode 8: Design of structures for earthquake resistance, Part 3: Assessment and retrofitting of buildings. *EN 1998-1 CEN*, Brussels, April 2004.
- [36] M. Kohrangi, D. Vamvatsikos, P. Bazzurro, Site dependence and record selection schemes for building fragility and regional loss assessment. *Earthquake Engineering and Structural Dynamics*, **46(10)**: 1625-1643, 2017.
- [37] N. Luco, C.A. Cornell, Structure-specific scalar intensity measures for near-source and ordinary earthquake ground motions. *Earthquake Spectra*, **23(2)**: 357-392, 2007.
- [38] F. Jalayer, J. Beck, F. Zareian, Analyzing the sufficiency of alternative scalar and vector intensity measures of ground shaking based on information theory. *Journal of Engineering and Mechanics*, **138(3)**: 307-316, 2012.
- [39] H. Ebrahimian, F. Jalayer, A. Lucchini, F. Mollaioli, G. Manfredi, Preliminary ranking of alternative scalar and vector intensity measures of ground shaking. *Bulletin of Earthquake Engineering*, **13(10)**: 2805-2840, 2015.
- [40] N. Shome, C.A. Cornell, Probabilistic seismic demand analysis of nonlinear structures. *Report No. RMS35*, Stanford University, CA, 1999: 320 pp.
- [41] FEMA P695. Quantification of Building Seismic Performance Factors. Washington (DC): *Federal Emergency Management Agency*; 2009.
- [42] H. Krawinkler, Van Nuys hotel building testbed report: exercising seismic performance assessment. *Technical Report PEER 2005/11*, Berkeley, USA.
- [43] A. Miano, H. Sezen, F. Jalayer, A. Prota, Performance Based Assessment and Retrofit of Non ductile Existing Reinforced Concrete Structures. *Structures Congress 2018: Blast, Impact Loading, and Response; and Research and Education - Selected Papers from the Structures Congress 2018*, Fort Worth, Texas, April 2018.
- [44] A. Miano, H. Sezen, F. Jalayer, A. Prota, Performance based comparison of different retrofit methods for reinforced concrete structures. *Proceedings of the 6<sup>th</sup> ECCOMAS Thematic Conference on Computational Methods in Structural Dynamics and Earthquake Engineering (COMPdyn)*, Rhodes, Greece, 15-17 June 2017.
- [45] H. Sezen, J.P. Moehle, Bond-slip behavior of reinforced concrete members. *Fib Symposium on Concrete Structures in Seismic Regions, CEB-FIP*, Athens, Greece, 2003.
- [46] M. Gaetani d'Aragona, M. Polese, E. Cosenza, A. Prota. Simplified assessment of maximum interstory drift for RC buildings with irregular infills distribution along the height. *Bulletin of Earthquake Engineering*, **17(2)**, 707-736, 2019.
- [47] F. Jalayer, R. De Risi, L. Elefante, G. Manfredi, Robust fragility assessment using Bayesian parameter estimation. *Congress on Recent Advances in Earthquake Engineering and Structural Dynamics 2013 (VEESD)*, Vienna, Austria, August 2013.

- [48] F. Jalayer, H. Ebrahimian, Updated robust reliability: considering record-to-record variability and uncertainty in modelling parameters. *Proceedings, 13<sup>th</sup> International Conference on Applications of Statistics and Probability in Civil Engineering (ICASP)*, Seoul, South Korea, May 2019.